

Variation with mass of $B(E3; 0_1^+ \rightarrow 3_1^-)$ transition rates in $A = 124 - 134$ even-mass xenon nuclei

W.F. Mueller^{1*}, M.P. Carpenter², J.A. Church^{1,3†}, D.C. Dinca^{1,3‡}, A. Gade¹, T. Glasmacher^{1,3}, D.T. Henderson², Z. Hu^{1§}, R.V.F. Janssens², A.F. Lisetskiy^{1¶}, C.J. Lister², E.F. Moore², T.O. Pennington², B.C. Perry^{1,3}, I. Wiedenhöver⁴, K.L. Yurkewicz^{1,3**}, V.G. Zelevinsky^{1,3}, and H. Zwahlen^{1,3}

¹National Superconducting Cyclotron Laboratory, Michigan State University, East Lansing, MI 48824-1321, USA

²Physics Division, Argonne National Laboratory, Argonne, IL 60439, USA

³Department of Physics and Astronomy, Michigan State University, East Lansing, MI 48824, USA and

⁴Department of Physics, Florida State University, Tallahassee, FL 32306, USA

(Dated: September 14, 2018)

$B(E3; 0_1^+ \rightarrow 3_1^-)$ transition matrix elements have been measured for even-mass $^{124-134}\text{Xe}$ nuclei using sub-barrier Coulomb excitation in inverse kinematics. The trends in energy $E(3^-)$ and $B(E3; 0_1^+ \rightarrow 3_1^-)$ excitation strengths are well reproduced using phenomenological models based on a strong coupling picture with a soft quadrupole mode and an increasing occupation of the intruder $h_{11/2}$ orbital.

PACS numbers: 21.10.Ky, 21.10.Re, 21.60.Ev, 21.60.Jz, 23.20.Lv, 27.60.+j, 29.40.Gx

Xenon isotopes with mass numbers from $A = 124$ to 134 are located in a transitional region of nuclei where their low-spin structure indicates an evolution from a weakly-deformed, γ -soft rotor to a vibrator. The positive-parity states of xenon nuclei in this region have been described within the framework of algebraic models [1, 2, 3, 4, 5, 6], of triaxial rotor-vibrator models [7], and using a pair-truncated shell-model description [8]. However, the low-spin, negative-parity structures have not been extensively investigated.

The properties of such negative-parity states can provide important information on the octupole degree of freedom. General features of collective octupole motion are still not well understood [9]. Specifically, the excitation energy and, more importantly, the $B(E3; 0_1^+ \rightarrow 3_1^-) = B(E3 \uparrow)$ transition probabilities for 3_1^- states are signatures of either octupole vibrational strength or static octupole deformation [10, 11].

While some information is available on the $B(E3 \uparrow)$ strength of nuclei in this mass region such as for Sn [12], Te [13], and Ba [14], the only data on octupole collectivity in xenon isotopes stems from an inelastic proton-scattering measurement on ^{136}Xe [15, 16]. The combination of soft quadrupole and octupole modes can make such nuclei as ^{129}Xe good candidates for the search of enhancement of the nuclear Schiff moment and atomic

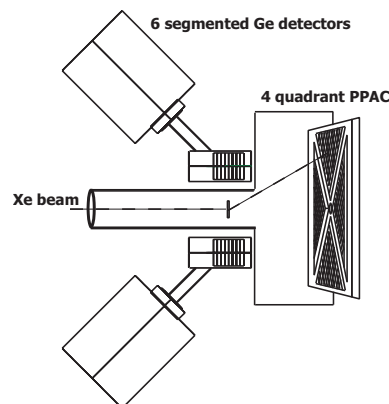


FIG. 1: Schematic drawing of the experimental setup used in the measurements.

electric dipole moment [17]. Here, we present the first determination of the $B(E3 \uparrow)$ rates in the chain of even-mass $^{124-134}\text{Xe}$ isotopes. These results are obtained under identical experimental conditions and compared to a global model [9] reproducing the trends of the $B(E3 \uparrow)$ strengths across the nuclear chart.

The xenon beams were delivered by the ATLAS accelerator at Argonne National Laboratory. The beam energies for the $A = 124 - 134$ even xenon isotopes were 555, 556, 553, 563, 571, and 579 MeV, respectively. These beams were directed to the experimental setup (see Fig. 1) where they impinged on a ^{58}Ni target with 1.1 mg/cm² thickness and an enrichment of $\geq 95\%$. Scattered xenon nuclei were detected in a large area, four quadrant, parallel-plate avalanche counter (PPAC). The entrance window was located 21.5 cm downstream from the target. The PPAC size was such that it covered laboratory scattering angles between 9° and 40°. The maximum laboratory scattering angle for the xenon nuclei was about 27°. Hence, it was possible to cover the most relevant scattering angular ranges.

*Present address: CANBERRA, 800 Research Parkway, Meriden, CT 06450.

†Present address: Lawrence Livermore National Laboratory, P.O. Box 808, L-414, Livermore, CA 94550.

‡Present address: American Science and Engineering, Inc., 829 Middlesex Turnpike, Billerica, MA 01821.

§Present address: Philips Medical Systems, 595 Miner Rd, Cleveland, OH 44143.

¶Present address: Theory Department, Planckstr. 1, 64291 Darmstadt, Germany.

**Present address: Fermilab, MS 206(WH 1E), Batavia IL 60510.

The γ rays from the reaction were observed with a setup of six germanium detectors from the MSU SeGA array [18]. These detectors were arranged in a barrel of 9.5 cm radius from the middle of the target to the center of the germanium crystals. In this arrangement, the array had an absolute photopeak efficiency of 6.0% at 1.3 MeV. The germanium detectors of SeGA are 32-fold segmented [18] and allow for a precise Doppler reconstruction of γ rays emitted by nuclei in flight. The total energy and timing information from each germanium detector were obtained from the central contact. The efficiency of the entire germanium array was determined with standard γ -ray calibration sources covering an energy range from 88 to 1836 keV. Corrections to this efficiency due to the summing of coincident events in individual detectors were estimated with the use of GEANT simulations [19] of the setup.

For each event, the arrival of a scattered particle in the PPAC was measured with respect to the ATLAS resonators frequency (rf). This allows for a clear separation of the small-angle ($<90^\circ$) and large-angle ($>90^\circ$) scattering in the center-of-mass due to the significant difference in the momentum (and consequently in time of flight) of the xenon nuclei in the two cases. Representative γ -ray spectra, gated on a partial angle range of forward (in the center-of-mass) scattered ^{128}Xe nuclei, are shown in Fig. 2.

For the analysis of data on ^{124}Xe and ^{126}Xe , the γ -ray events were sorted into spectra corresponding to five equal divisions of scattering angles between 10.6° and 16.0° in the laboratory frame. For the heavier Xe isotopes, the five angle cuts were between 12.7° and 19.0° . It should be noted that in all cases the condition $r_{min} > (1.25(A_t^{1/3} + A_p^{1/3}) + 5)$ [fm] was satisfied, excluding nuclear contributions to the excitation process [20].

The γ -ray intensities corrected for the efficiency were determined for each scattering angle. From these, level schemes were constructed by comparing the measured energies to previously known data [21, 22, 23, 24, 25, 26] with verification that the relative intensities were consistent with Coulomb excitation. In cases where new γ rays were identified, placements are proposed based on γ - γ coincidences.

Excited states with confirmed spins of $3\hbar$ have been clearly identified in ^{124}Xe , ^{126}Xe , and ^{128}Xe at 1898.0 [5], 2004.8 [27], and 2138.7 keV [3], respectively. While the negative parity for these states is suggested, there is circumstantial evidence to support such an assignment in each case.

The observation of a 3^- state in ^{130}Xe has not been reported previously. In the present experiment, several candidate γ -ray transitions were observed. Five transitions were found to feed the 2_1^+ state in ^{130}Xe and can be viewed as candidates for decays from a 3^- state. Two of these γ rays at 1687 and 1707 keV have been previously observed to feed the first 2^+ level following ^{130}Cs electron capture decay [28]. However, the reported $\log ft$ values are not consistent with the forbidden decay that would

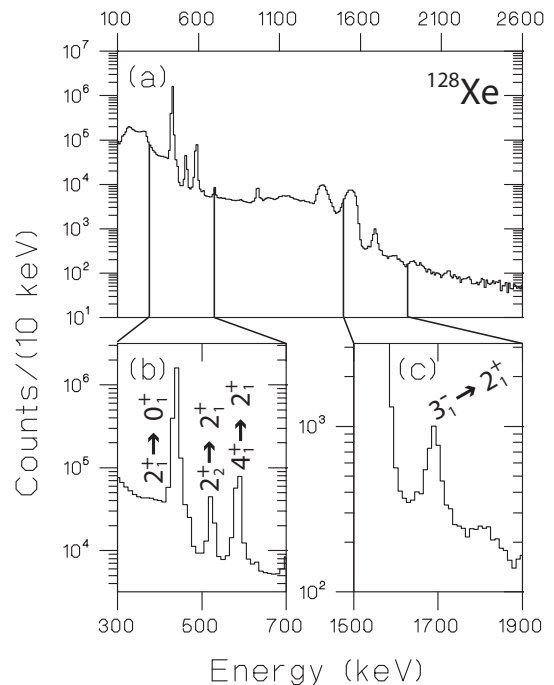


FIG. 2: Representative γ -ray spectra for the $^{128}\text{Xe} + ^{58}\text{Ni}$ reaction in coincidence with scattered ^{128}Xe . The spectra are gated on forward scattering angles from 17.8° to 19.0° in the laboratory frame. Panel (a) represents the energy range of interest. Panel (b) shows peaks corresponding to the $2_1^+ \rightarrow 0_1^+$, $2_2^+ \rightarrow 2_1^+$, and $4_1^+ \rightarrow 2_1^+$ γ -ray transitions. Panel (c) highlights the $3_1^- \rightarrow 2_1^+$ transition of interest in the present work.

be expected between the 1^+ ground state of ^{130}Cs and a 3^- state. Of the three remaining γ rays with respective energies of 1742, 1896, and 2033 keV, the most intense—after efficiency corrections—is the 1742 keV transition. For $^{124,126,128}\text{Xe}$, the $3^- \rightarrow 2^+$ transition was the dominant γ ray in the spectrum above 1400 keV (see e.g. Fig. 2). Consequently, the 1742 keV transition is identified as a candidate for the decay of the 3_1^- state. Based on sum-energy and intensity-balance considerations, an observed 1073 keV γ ray is placed feeding the 4_1^+ state from this same level. It should be noted that, if this assignment is in error, the $B(E3; 0_1^+ \rightarrow 3_1^-)$ strength would be less than the value presented below.

A candidate 3^- state in ^{132}Xe was proposed at an excitation energy of 2469 keV by Gelletly *et al.* [29], from the decay by a 1801 keV γ ray that is also observed in the present experiment. Unlike the lighter Xe nuclei, where the strongest decay branch from the 3^- level occurs to the 2_1^+ state, the 2469 keV level in ^{132}Xe has rather significant de-excitation branches to the 4_1^+ , 2_2^+ , and 2_3^+ states.

In ^{134}Xe , a candidate for the 3^- level has not yet been identified. In addition, none of the γ rays identified in the present experiment are consistent with expectations for a 3^- state (i.e., a γ ray feeding the 2_1^+ state with an energy between 1500 to 2000 keV). Consequently, an energy for

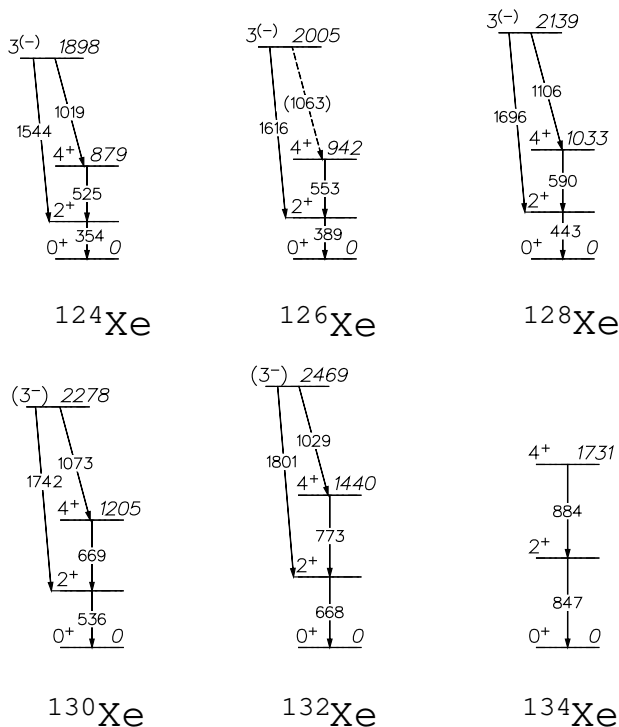


FIG. 3: Partial decay schemes for even $^{124-134}\text{Xe}$ isotopes. Shown for each isotope are the experimental (Exp.) 0_1^+ , 2_1^+ , and 4_1^+ levels, as well as the proposed 3_1^- state with corresponding γ -ray transitions (dashed transitions correspond to known γ rays that are not observed in the present measurements).

the 3^- state is not proposed for ^{134}Xe . An upper limit on the $B(E3; 0_1^+ \rightarrow 3_1^-)$ strength was determined assuming that the excitation energy for the 3^- state is between 2400 and 3000 keV.

For the determination of the electromagnetic transition matrix elements, the angle-dependent γ -ray yields were analyzed using the Coulomb excitation code GOSIA [30, 31]. This code combines the semi-classical theory of multiple Coulomb excitation [32] and the measured γ -ray de-excitation patterns with a numerical least-squares analysis to determine the electromagnetic matrix elements from the experimental γ -ray yields. In addition to the γ -ray yields determined in the present experiments, the previously observed γ -ray branching ratios and multipole mixing ratios for relevant transitions were used when possible as additional information to constrain the determination of the matrix elements further. For those cases where a branching ratio is not known (e.g. the 3^- state in ^{130}Xe), the ratio is fit based solely on the presently measured data.

All observed γ -ray yields were used in the calculation of the transition matrix elements in each of the Xe nuclei. This includes transitions not presented in Fig. 3. γ -ray branching ratios for transitions from the 3^- states are listed in Table I. The determination of the $M(E3)$ transition matrix elements was carried out using the

TABLE I: γ -ray branching ratios for transitions from the 3^- states for different Xe isotopes.

	$E(3^-)$ (keV)	E_f (keV)	E_γ (keV)	Branching ratio
^{124}Xe	1898*	354	1544	100(13)
		879	1019 [†]	16(8)
^{126}Xe	2005	389	1616	100(17)
		942	1063	21(1)
^{128}Xe	2139	443	1696	100(3)
		1033	1106	
^{130}Xe	2278	536	1742 [†]	54(10)
		1205	1073 [†]	100(26)
^{132}Xe	2469	668	1801	56(11)
		1440	1029	69(8)
		1298	1171	11(2)
		1963	506	<6.4
		1986	483	100(9)
		2040	429	8(2)

* Negative parity proposed by the present work.

[†] γ -ray not previously reported.

method described in Ref. [14]. Specifically, the $M(E1)$ transition matrix elements (e.g. $M(E1; 2_1^+ \rightarrow 3^-)$ and $M(E1; 4_1^+ \rightarrow 3^-)$) were set equal to a total strength of 10^{-4} W.u., with relative strengths adjusted to reproduce the branching ratios (if known). $E1$ strengths of 10^{-4} W.u. are typical for this mass region (see e.g. Ref. [35]). The static quadrupole moments for the 3^- states ($Q(3^-)$) were set to zero. The $M(E3; 0_1^+ \rightarrow 3^-)$ matrix element (as well as the matrix elements of other transitions) were then varied to reproduce the observed yields as a function of the xenon scattering angle for the $3^- \rightarrow 2_1^+$ and other γ -ray transitions seen in this work. To check the sensitivity of the calculation with respect to correlations between the extracted $E1$ and $E3$ strengths, the $M(E1)$ parameters were increased and decreased by as much as a factor of ten, and in all cases the change of the extracted $M(E3)$ matrix element was found to be less than 2.5%. This indicates, that in the excitation strength of the 3_1^- state, the one-step $E3$ strength dominates over two-step excitations, leading to a high experimental sensitivity for $B(E3)$ strength. Additionally, variations of the $Q(3^-)$ moment by ± 0.5 eb resulted in changes in the extracted values of less than $\pm 5\%$ for all cases. These uncertainties are included in the overall errors of the experimental results quoted in this work.

The deduced $B(E2; 0_1^+ \rightarrow 2_1^+)$ and $B(E3; 0_1^+ \rightarrow 3_1^-)$ rates are presented in Table II. Also given are the $B(E2; 0_1^+ \rightarrow 2_1^+)$ values from the references listed in the table. There is good general agreement between the previously measured $B(E2; 0_1^+ \rightarrow 2_1^+)$ values and those determined in the present work.

Figure 4 shows the experimental and calculated exci-

TABLE II: Reduced transitions rates for $A = 124 - 136$ even Xe nuclei. Those columns listed “present” are the transition rates from the measurements reported here (in both e^2b^λ and Weisskopf units), while “previous” are $B(E2 \uparrow)$ rates from the references listed in square brackets.

	$B(E2; 0_1^+ \rightarrow 2_1^+)$			$B(E3; 0_1^+ \rightarrow 3_1^-)$	
	present		previous	present	
	(e^2b^2)	(W.u.)	(W.u.)	(e^2b^3)	(W.u.)
^{124}Xe	1.12_{-9}^{+12}	60.8_{-50}^{+62}	57.8_{-14}^{+15} [33]	0.091(10)	14.3(16)
^{126}Xe	1.02_{-6}^{+13}	54.2_{-30}^{+70}	40(14) [22]	0.085(13)	13(2)
^{128}Xe	0.825_{-12}^{+11}	42.6_{-64}^{+54}	40.2(55) [23]	0.083(11)	12(2)
^{130}Xe	0.585_{-6}^{+9}	30.0_{-28}^{+44}	37.2(17) [34]	0.033(9)	4.7(13)
^{132}Xe	0.499_{-32}^{+36}	25.0_{-16}^{+18}	23.7(6) [34]	0.016(6)	2.1(9)
^{134}Xe	0.322_{-16}^{+41}	15.8_{-8}^{+20}	14.7(1) [34]	<0.011	<1.5

tation energies $E(3_1^-)$ and $B(E3 \uparrow)$ strengths. It can be seen that the excitation energy of the 3_1^- state increases smoothly from 1898 keV in ^{124}Xe to 2469 keV in ^{132}Xe with the $B(E3 \uparrow)$ strength gradually decreasing towards ^{134}Xe . As discussed in [9], collective octupole motion in such nuclei is strongly influenced by quadrupole softness. Qualitatively speaking, the octupole motion proceeds on the background of a slowly changing dynamic quadrupole deformation. Simple semi-microscopic arguments predict the energy of the octupole phonon to be correlated with that of the quadrupole phonon as

$$E(3_1^-) = E_0 - \frac{B^2}{E(2_1^+)}. \quad (1)$$

In Fig. 4, our experimental results are compared to eq. (1), where $B = 0.7$ MeV, $E_0 = 3.275$ MeV (from the energy of the 3_1^- state in the closed-shell nucleus ^{136}Xe) and $E(2_1^+)$ is in MeV.

The global behavior of the octupole strength throughout the nuclear chart was described in [9] by the expression of the type

$$B(E3 \uparrow) = \kappa Z^2 A^{1/3} \frac{1}{E(3_1^-)} \xi \quad [e^2b^3] \quad (2)$$

using the universal Z - and A -dependence, the parameter κ setting the global scale and the local parameter ξ depending on pairing and details of the shell structure. For xenon nuclei, the 3_1^- state is likely dominated by $\Delta j = \Delta l = 3$, $d_{5/2} \otimes h_{11/2}$ correlations. The occupation of the $h_{11/2}$ orbital gradually increases for heavier xenon isotopes until ^{136}Xe , where the $\nu h_{11/2}$ configuration is completely filled ($N = 82$) and thus octupole correlations involving this orbit are blocked. Using $\kappa = 1.4 \cdot 10^{-5} e^2b^3$, the value close to the average value chosen in [9], $E(3_1^-)$ in MeV, and the occupation factor $\xi = (82 - N)/12$ as a measure of the availability of the $\nu h_{11/2}$ orbit to form octupole correlations, we come to the fit of Fig. 4. Detailed microscopic calculations would require a theory taking into account strong quadrupole anharmonicity, coupling between the modes beyond the conventional

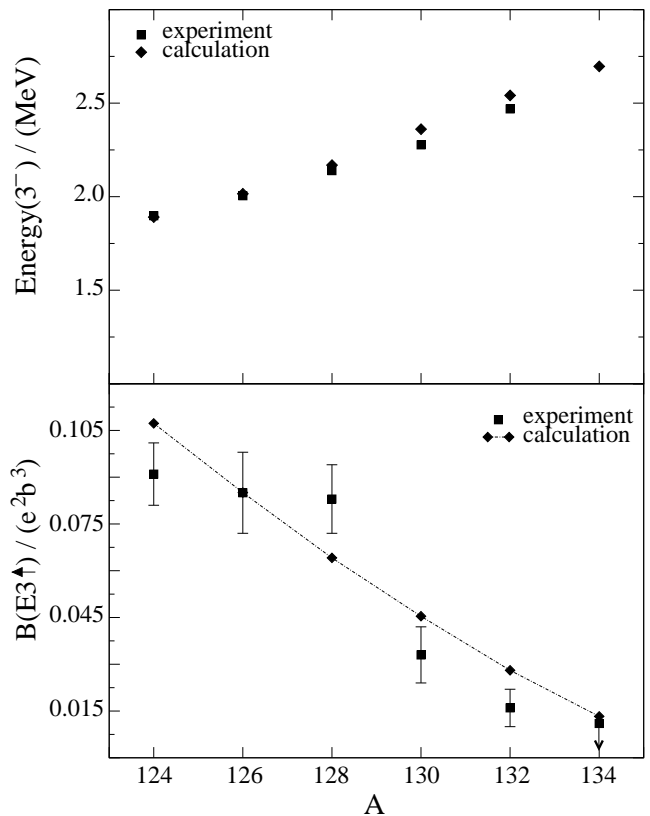


FIG. 4: Experimental results compared to phenomenological calculations outlined in the text.

random phase approximation, and possible fragmentation of the octupole strength.

The $N = 82$ nucleus ^{136}Xe was not a subject of the present study. The first 3_1^- state has been established at 3275 keV and a $B(E3)$ value of 17(5) W.u. was determined in inelastic proton scattering [15]. The octupole strength observed in this semi-magic nucleus is not related to the octupole correlations formed with participation of the $h_{11/2}$ orbit and is thus outside our phenomenological description of the properties of the lighter Xe isotopes. The growth of octupole strength is also known for other magic nuclei, for example for ^{40}Ca [16].

The data presented here represent the first determination of the $B(E3; 0_1^+ \rightarrow 3_1^-)$ values in a chain of even-even $^{124-134}\text{Xe}$ nuclei. The trends in energy $E(3_1^-)$ and $B(E3; 0_1^+ \rightarrow 3_1^-)$ excitation strengths are well reproduced using phenomenological models with the universal A - and Z -dependence. The smoothly increasing excitation energy of the 3_1^- states from ^{124}Xe to ^{134}Xe and the decreasing $B(E3 \uparrow)$ strength can be understood, at least qualitatively, as being associated with the presence of the soft quadrupole mode of the mean field and the decreased availability of the $\nu h_{11/2}$ orbital for the generation of octupole correlations.

The authors thank the staff of ATLAS for providing high-quality xenon beams. W.F. Mueller thanks D. Cline and C. Y. Wu for significant assistance in us-

ing the GOSIA code and acknowledges fruitful discussions with P.D. Cottle and R.M. Rommingen. A.G. acknowledges support from Professor P. von Brentano and the University of Cologne. This work was supported by the National Science Foundation under grant numbers

PHY-0110253, PHY-9875122, PHY-0244453, and by the United States Department of Energy, Office of Nuclear Physics, under contract numbers W-31-109-ENG-38 and DE-FG02ER41220.

-
- [1] R.F. Casten and P. von Brentano, *Phys. Lett.* **152**, 22 (1985).
- [2] V.G. Zelevinsky, In: *New Trends in Nuclear Collective Dynamics*, Genshikaku Kenkyu (Tokyo) **35**, 21 (1991); see also discussion in G.F. Bertsch, *Nucl. Phys.* **A574**, 169c (1994).
- [3] U. Neuneyer *et al.*, *Nucl. Phys. A* **607**, 299 (1996).
- [4] A. Gade *et al.*, *Nucl. Phys. A* **665**, 268 (2000).
- [5] V. Werner *et al.*, *Nucl. Phys. A* **692**, 451 (2001).
- [6] X.-W. Pan *et al.*, *Phys. Rev. C* **53**, 715 (1996).
- [7] U. Meyer *et al.*, *Nucl. Phys. A* **641**, 321 (1998).
- [8] N. Yoshinaga and K. Higashiyama, *Phys. Rev. C* **69**, 054309 (2004).
- [9] M.P. Metlay, J.L. Johnson, J.D. Canterbury, P.D. Cottle, C.W. Nestor, Jr., S. Raman and V.G. Zelevinsky, *Phys. Rev. C* **52**, 1801 (1995).
- [10] R.H. Spear and W.N. Catford, *Phys. Rev. C* **41**, 1351 (1990).
- [11] W. Nazarewicz *et al.*, *Nucl. Phys. A* **429**, 269 (1984).
- [12] N.-G. Jonsson *et al.*, *Nucl. Phys. A* **371**, 333 (1981).
- [13] M. Matoba *et al.*, *Nucl. Phys. A* **237**, 260 (1975).
- [14] S. M. Burnett *et al.*, *Nucl. Phys. A* **432**, 514 (1985).
- [15] S. Sen *et al.*, *Phys. Rev. C* **6**, 2201 (1972).
- [16] T. Kibédi and R.H. Spear, *At. Data & Nucl. Data Tables* **80**, 35 (2002).
- [17] V.V. Flambaum and V.G. Zelevinsky, *Phys. Rev. C* **68**, 035502 (2003).
- [18] W.F. Mueller *et al.*, *Nucl. Inst. and Meth. A* **466**, 492 (2001).
- [19] GEANT-detector description and simulation tool, version 3.21, Technical Report W5013, CERN (1994).
- [20] D. Cline, *Ann. Rev. Nucl. Part. Sci.* **36**, 683 (1986).
- [21] H. Iimura *et al.*, *Nucl. Data Sheets* **80**, 895 (1997).
- [22] J. Katakura and K. Kitao, *Nucl. Data Sheets* **97**, 765 (2002).
- [23] M. Kanbe and K. Kitao, *Nucl. Data Sheets* **94**, 227 (2001).
- [24] B. Singh, *Nucl. Data Sheets* **93**, 33 (2001).
- [25] Yu.V. Sergeenkov, *Nucl. Data Sheets* **65**, 277 (1992).
- [26] A.A. Sonzogni, *Nucl. Data Sheets* **103**, 1 (2004).
- [27] F. Seiffert *et al.*, *Nucl. Phys. A* **554**, 287 (1993).
- [28] P.K. Hopke *et al.*, *Phys. Rev. C* **8**, 745 (1973).
- [29] W. Gelletly *et al.*, *Phys. Rev. C* **3**, 1678 (1971).
- [30] T. Czosnyka *et al.*, *Nucl. Phys. A* **458**, 123 (1986).
- [31] T. Czosnyka *et al.*, GOSIA users manual, NSRL-305, 1991.
- [32] K. Alder and A. Winther, *Electromagnetic Excitation Theory of Coulomb Excitation with Heavy Ions*, North Holland, Amsterdam (1975).
- [33] B. Saha *et al.*, *Phys. Rev. C* **70**, 034313 (2004).
- [34] G. Jakob *et al.*, *Phys. Rev. C* **65**, 024316 (2002).
- [35] P.D. Cottle, *Phys. Rev. C* **47**, 1529 (1993).